Salidroside mediates apoptosis and autophagy inhibition in concanavalin A-induced liver injury

JIAO FENG[1*], PEIQIN NIU[2*], KAN CHEN[1*], LIWEI WU[1], TONG LIU[1], SHIZAN XU[3], JINGJING LI[1], SAINAN LI[1], WENWEN WANG[1], XIYA LU[1], QIANG YU[3], NING LIU[3], LING XU[4], FAN WANG[5], WEIQI DAI[6,7], YUJING XIA[1], XIAOMING FAN[8] and CHUANYONG GUO[1]

[1]Department of Gastroenterology, Shanghai Tenth People's Hospital, Affiliated to Tongji University School of Medicine, Shanghai 200072; [2]Department of Gastroenterology, Shanghai Tenth People's Hospital Chongming Branch, Tongji University School of Medicine, Shanghai 202157; [3]School of Clinical Medicine of Nanjing Medical University, Shanghai Tenth People's Hospital, Shanghai 200072; [4]Department of Gastroenterology, Shanghai Tongren Hospital, Shanghai Jiaotong University School of Medicine, Shanghai 200336; [5]Department of Oncology, Shanghai General Hospital, Shanghai Jiaotong University School of Medicine, Shanghai 200080; [6]Department of Gastroenterology; [7]Shanghai Institute of Liver Diseases, Zhongshan Hospital of Fudan University, Shanghai 200032; [8]Department of Gastroenterology, Jinshan Hospital of Fudan University, Shanghai 201508, P.R. China

Received October 11, 2017; Accepted February 22, 2018

DOI: 10.3892/etm.2018.6053

Abstract. Salidroside (Sal) is a glycoside extract from *Rhodiola rosea* L. with anti-inflammatory, antioxidant, anti-cancer and cardioprotective properties. The present study explored the protective effects and the possible mechanisms of Sal on concanavalin A (ConA)-induced liver injury in mice. Balb/C mice were divided into five groups: Normal control (injected with normal saline), ConA (25 mg/kg), Sal (10 mg/kg) +ConA, Sal (20 mg/kg) + ConA (Sal injected 2 h prior to ConA injection) and Sal (20 mg/kg) only. The serum levels of liver enzymes, pro-inflammatory cytokines, and apoptosis- and autophagy-associated marker proteins were determined at 2, 8 and 24 h after ConA injection. LY294002 was further used to verify whether the phosphoinositide 3-kinase (PI3K)/Akt pathway was activated. Primary hepatocytes were isolated to verify the effect of Sal *in vitro*. The results indicated that Sal was a safe agent to reduce pathological damage and serum liver enzymes in ConA-induced liver injury. Sal suppressed inflammatory reactions in serum and liver tissues, and activated the PI3K/Akt signaling pathway to inhibit apoptosis and autophagy *in vivo* and *in vitro*, which could be reversed by LY294002. In conclusion, Sal attenuated ConA-induced liver injury by modulating PI3K/Akt pathway-mediated apoptosis and autophagy in mice.

Correspondence to: Dr Xiaoming Fan, Department of Gastroenterology, Jinshan Hospital of Fudan University, 1508 Longhang Road, Jinshan, Shanghai 201508, P.R. China
E-mail: xiaomingfan57@hotmail.com

Dr Chuanyong Guo, Department of Gastroenterology, Shanghai Tenth People's Hospital, Affiliated to Tongji University School of Medicine, 301 Middle Yanchang Road, Jing'an, Shanghai 200072, P.R. China
E-mail: guochuanyong@hotmail.com

*Contributed equally

Key words: salidroside, concanavalin A, liver injury, apoptosis, autophagy, phosphoinositide 3-kinase/Akt, LY294002

Introduction

Autoimmune hepatitis (AIH) is an increasingly serious human health problem worldwide (1). Although the precise etiology of AIH remains unknown, it is thought to be a multifactorial polygenic disorder caused by genetic and environmental factors (1-3). AIH is characterized by increased serum aminotransferase, pro-inflammatory cytokine and immunoglobulin levels (1). The standard treatment for AIH consists of steroids, immunosuppressive medications and liver transplantation. This treatment delays disease progression and exacerbation, but it is associated with certain side effects, particularly Cushingoid changes (1-4). Therefore, novel approaches to the treatment of AIH are needed.

Concanavalin A (ConA), which is extracted from the jack bean *Canavalia ensiformis*, is a lectin with agglutination and mitogenic properties. It can bind to sugar residues on the surface of multiple cell types (5-7). ConA is able to activate T cells, leading to the activation of inflammatory reactions and the release of inflammatory cytokines, including interleukin (IL)-1β, IL-6, tumor necrosis factor-α (TNF-α) and interferon-γ (IFN-γ) (8). Tiegs *et al* (5) explored the possibility that ConA induces hepatitis. The results indicated that ConA-induced acute liver injury could serve as a suitable animal model of AIH, since it closely mimicked the pathogenetic mechanisms and pathological changes of patients with AIH.

Previously, researchers have demonstrated that apoptosis and autophagy are involved in the pathogenesis of

ConA-induced liver injury (9-15). Apoptosis is type I programmed cell death caused by endogenous or exogenous signals, leading to the elimination of dead cells without generating inflammatory activity. Apoptosis is regarded as a double-edged sword, as it can avoid inflammatory responses, but it can also lead to tissue damage when over-activated (15,16). Autophagy is a process by which cells eliminate discarded components by enveloping them into autophagosomes and targeting them for lysosomal degradation (9,17). Autophagy is beneficial to the survival of cells because it removes unwanted cellular substances and provides energy under starvation conditions. However, it can also lead to cell death if the process is excessively activated (9,18). Apoptosis and autophagy are overactivated in ConA-induced liver injury and contribute to liver injury (11).

Salidroside (Sal) is a phenylpropanoid glycoside extracted from *Rhodiola rosea* L. (19). In traditional Chinese medicine, it is thought to enhance cognition and physical performance for prolonged periods (20). Previous studies have reported that Sal exhibits numerous bioactive properties, including anti-inflammatory, antioxidant, anticancer, anti-depression, anti-fatigue and cardioprotective effects (21-25). Sal was demonstrated to exert its protective effect by regulating the apoptosis pathway (26,27). Hu *et al* (19) reported that Sal attenuates ConA-induced hepatitis by modulating cytokine secretion and lymphocyte migration in mice.

Based on these previous findings, in the present study, the protective effect of Sal on ConA-induced liver injury was investigated in mice and its underlying mechanisms were explored. It was hypothesized that Sal ameliorates ConA-induced liver injury by modulating inflammation, apoptosis and autophagy through the phosphoinositide 3-kinase (PI3K)/Akt pathway.

Materials and methods

Reagents. Sal, ConA, LY294002, collagenase and D-Hanks buffer were purchased from Sigma-Aldrich (Merck KGaA, Darmstadt, Germany). TNF-α was obtained from PeproTech, Inc. (Rocky Hill, NJ, USA). Alanine aminotransferase (ALT) and aspartate aminotransferase (AST) microplate test kits were obtained from Nanjing Jiancheng Bioengineering Institute (Nanjing, China). Enzyme-linked immunosorbent assay (ELISA) kits for IL-6 (cat. no. MEC1008) and TNF-α (cat. no. MEC1003) were purchased from Anogen (Mississauga, ON, Canada). The cell counting kit-8 (CCK8) was purchased from Dojindo Molecular Technologies, Inc. (Kumamoto, Japan). Oligonucleotide primers were synthesized by Generay Biotech Co., Ltd. (Shanghai, China). The primary antibodies used in this study are listed in Table I. The PrimeScript RT Reagent kit and SYBR Premix Ex Taq were obtained from Takara Biotechnology Co., Ltd. (Dalian, China). The TUNEL apoptosis assay kit was provided by Roche Diagnostics (Basel, Switzerland). All other reagents were of analytical grade.

Animals and treatment. A total of 114 male Balb/c mice (6-8 weeks old, 23±2 g) were purchased from Shanghai SLAC Laboratory Animal Co., Ltd. (Shanghai, China). The mice were housed in a clean room maintained at 24±2˚C and 55% humidity with a 12/12-h light/dark cycle, with free access to food and water. The mice were used for three separate experiments: i) Establishment of the ConA model (n=78, randomly divided into five groups); ii) evaluation of treatment with LY294002 (n=24, randomly divided into four groups) and iii) isolation of primary hepatocytes (n=12). The study was approved by the Animal Care and Use Committee of Tongji University (Shanghai, China), and was performed in accordance with the National Institutes of Health Guide for the Care and Use of Laboratory Animals and the ARRIVE guidelines (28,29). No mice died or became severely ill prior to the end of the experiment. Efforts were made to minimize the pain and suffering of the mice throughout the study.

Establishment of the ConA model. Sal was diluted with normal saline and injected intraperitoneally 2 h before the injection of ConA, which was administered according to the pharmacokinetics of Sal (30). The doses of Sal were 10 and 20 mg/kg, according to a previous study (31). ConA was dissolved in normal saline at a concentration of 5 mg/ml and injected via the tail vein at a dose of 25 mg/kg to induce acute hepatic injury. The experiment included 78 mice randomly divided into five groups as follows: i) Normal control (NC), n=18, injected with vehicle (saline); ii) ConA, n=18, injected with ConA (25 mg/kg) only; iii) Sal 20 mg/kg, n=6, injected with Sal only; iv) Sal (10 mg/kg) + ConA, n=18, injected with 10 mg/kg Sal 2 h before injection of ConA; v) Sal (20 mg/kg) + ConA, n=18, injected with 20 mg/kg Sal 2 h before injection of ConA.

A total of 6 mice were sacrificed randomly at 2, 8 and 24 h after ConA injection (mice in group 3 were sacrificed at 24 h after Sal treatment). The mice were sacrificed by cervical dislocation under anesthesia with sodium pentobarbital (40 mg/kg, 1.25%, intraperitoneal) (Nembutal; cat. no. P3761; Sigma-Aldrich; Merck KGaA) (13,32,33). Blood samples were collected by removing the eyes and the liver tissue was isolated. The serum was separated by centrifugation at 4,500 x g at 4˚C for 10 min. The serum and liver tissues were stored at -80˚C.

Evaluation of treatment with LY294002. LY294002, a specific inhibitor of PI3K, was used to create another group of experiments to investigate whether the protective effect of Sal was associated with the PI3K/Akt pathway. A total of 24 four mice were randomly divided into four groups (n=6): i) NC, ii) ConA, iii) Sal (20 mg/kg) + ConA, iv) Sal (20 mg/kg) + LY294002 (40 mg/kg) + ConA. LY294002 was diluted in 10% dimethyl sulfoxide and 90% PBS, and was injected intraperitoneally 2 h before ConA injection (34). All mice in each group were sacrificed at 8 h after ConA injection. The mice were sacrificed by cervical dislocation under anesthesia with sodium pentobarbital (40 mg/kg, 1.25%, intraperitoneal) Blood samples were collected by removing the eyes and the liver tissue was isolated. The serum was separated by centrifugation at 4,500 x g at 4˚C for 10 min. The serum and liver tissues were stored at -80˚C.

Biochemical assays. The serum levels of ALT and AST were detected with an automated chemical analyzer (Olympus AU1000, Olympus Corporation, Tokyo, Japan). The serum inflammatory cytokines IL-6 and TNF-α were measured using ELISA kits, according to the manufacturer's protocol.

Table I. Primary antibodies used in the current study.

Antibody	Type	Species	Targeted species	Dilution ratio (western blot/IHC)	Supplier	Catalog number
β-actin	Mono	M	H, M, R	1:1,000	CST	#3700
IL-1β	Mono	R	M	1:1,000	CST	#12507
IL-6	Poly	R	H, M, R	1:1,000/1:200	PT	21865-1-AP
TNF-α	Mono	M	H, M, R	1:1,000/1:200	PT	60291-1-Ig
Bcl-2	Mono	M	H, M	1:500/1:200	Ab	ab692
Bax	Poly	R	H, M, R	1:1,000/1:200	PT	60267-1-Ig
Caspase-3	Poly	R	H, M, R	1:1,000	PT	19677-1-AP
Caspase-9	Mono	M	H, M, R	1:1,000	PT	66169-1-Ig
Beclin-1	Poly	R	H, M, R	1:1,000/1:200	PT	11306-1-AP
LC3	Poly	R	H, M, R	1:500/1:200	PT	14600-1-AP
p62	Poly	R	H, M, R	1:1,000	PT	55274-1-AP
PI3K	Poly	R	H, M, R	1:1,000/1:200	PT	20584-1-AP
Akt	Mono	M	H, M, R	1:2,000	PT	60203-2-Ig
p-Akt	Mono	M	H, M, R	1:1,000/1:200	PT	66444-1-Ig

IHC, immunohistochemistry; IL, interleukin; TNF, tumor necrosis factor; Bcl-2, B-cell lymphoma-2; Bax, Bcl-2 associated X protein; LC3, microtubule-associated protein 1A/1B-light chain 3; PI3K, phosphoinositide 3-kinase; p-, phosphorylated; H, human; M, mouse; R, rabbit; CST, Cell Signaling Technology, Inc. (Danvers, MA, USA); PT, ProteinTech Group, Inc. (Chicago, IL, USA); Ab, Abcam (Cambridge, MA, USA).

Histopathology. The middle portion of the left lobe of the liver was excised and fixed in 4% paraformaldehyde at 4˚C for ≥24 h. Then, the tissues were paraffin-embedded, cut into 3-μm thick sections, and stained with hematoxylin for 10 min and eosin for 5 min to observe the degree of inflammation and tissue damage by light microscopy. All procedures were performed at 37˚C. The ratios of necrotic and inflammatory areas to total areas were calculated using Image-Pro Plus software 6.0 (Media Cybernetics, Rockville, MD, USA).

Reverse transcription-quantitative polymerase chain reaction (RT-qPCR). Total RNA was extracted from liver tissues using TRIzol reagent (Thermo Fisher Scientific, Inc., Waltham, MA, USA) and transcribed into total complementary DNA (cDNA) using an RT kit. The RT conditions were: 37˚C for 15 min, 85˚C for 5 sec and 4˚C until removal of the RT products. Then, cDNA was used as a template for qPCR with SYBR Premix Ex Taq, according to the manufacturer's protocol. The qPCR conditions were: 95˚C for 30 sec, 95˚C for 5 sec and 60˚C for 30 sec (40 cycles). The qPCR results were detected with a 7900HT Fast PCR system (Applied Biosystems; Thermo Fisher Scientific, Inc.). The qPCR results were quantified using the $2^{-\Delta\Delta Cq}$ method (35). The primers used for qPCR are listed in Table II.

Western blot analysis. Western blot analysis was used to determine the differential expression of proteins of interest. Total protein was extracted from cryopreserved liver tissues using radioimmunoprecipitation assay buffer (Nanjing KeyGen Biotech Co., Ltd., Nanjing, China), and the protein concentration was detected with a bicinchoninic acid assay (Nanjing KeyGen Biotech Co., Ltd.). Proteins (80 μg/lane) were separated by 7.5-12.5% sodium dodecyl sulfate polyacrylamide gel electrophoresis according to standard protocols and then transferred onto polyvinylidene fluoride membranes using the wet transfer method. Then, membranes were blocked with 5% nonfat milk dissolved in PBS to block non-specific binding sites at room temperature for 1 h, followed by incubation with monoclonal primary antibodies overnight at 4˚C (Table I). β-actin was used as an internal loading control for protein normalization. On the second day, the membranes were washed with PBS containing 0.1% Tween three times (10 min/wash) and then incubated with goat anti-mouse (cat. no. 926-68020) or goat anti-rabbit (cat. no. 926-32211) (both LI-COR Biosciences, Lincoln, NE, USA; 1:2,000) secondary antibodies for 1 h at 37˚C. After three washes, the membranes were imaged and the density was measured using the Odyssey two-color infrared laser imaging system and software 1.0 (LI-COR Biosciences).

Immunohistochemistry. The prepared paraffin-embedded 3-μm liver sections were dewaxed in a baking oven at 60˚C for 20 min, then rehydrated with xylene and a descending alcohol series. The sections were treated using an antigen retrieval technique consisting of heating in a water bath at 95˚C for 10 min and incubation in 3% hydrogen peroxide solution for 20 min at 37˚C to block endogenous peroxidase activity. The nonspecific binding sites were blocked with 5% bovine serum albumin (Nanjing KeyGen Biotech Co., Ltd.) at 37˚C for 20 min, then at room temperature for 10 min. Then, the liver sections were incubated overnight at 4˚C with the primary antibodies (Table I). The next day, after incubation with polymer rabbit-mouse HRP conjugated secondary antibodies (Dako; Agilent Technologies, Inc., Santa Clara, CA, USA; cat. no. K5007; 1:1) for 30 min at room temperature, the liver sections were analyzed with a diaminobenzidine kit to detect antibody binding. The sections were then counterstained with hematoxylin at room temperature for 30 sec, dehydrated with a graded ethanol and xylene series, and mounted with Entellan

Table II. Primers used in quantitative polymerase chain reaction.

Gene	Forward/ reverse	Primer sequence (5'-3')
β-actin	Forward	GGCTGTATTCCCCTCCATCG
	Reverse	CCAGTTGGTAACAATGCCATGT
IL-1β	Forward	CGATCGCGCAGGGGCTGGGCGG
	Reverse	AGGAACTGACGGTACTGATGGA
IL-6	Forward	CTGCAAGAGACTTCCATCCAG
	Reverse	AGTGGTATAGACAGGTCTGTTGG
TNF-α	Forward	CAGGCGGTGCCTATGTCTC
	Reverse	CGATCACCCCGAAGTTCAGTAG
Bcl-2	Forward	GCTACCGTCGTCGTGACTTCGC
	Reverse	CCCCACCGAACTCAAAGAAGG
Bax	Forward	AGACAGGGGCCTTTTTGCTAC
	Reverse	AATTCGCCGGAGACACTCG
Caspase-3	Forward	CTCGCTCTGGTACGGATGTG
	Reverse	TCCCATAAATGACCCCTTCATCA
Caspase-9	Forward	GGCTGTTAAACCCCTAGACCA
	Reverse	TGACGGGTCCAGCTTCACTA
Beclin-1	Forward	ATGGAGGGGTCTAAGGCGTC
	Reverse	TGGGCTGTGGTAAGTAATGGA
LC3	Forward	GACCGCTGTAAGGAGGTGC
	Reverse	AGAAGCCGAAGGTTTCTTGGG
p62	Forward	GAGGCACCCCGAAACATGG
	Reverse	ACTTATAGCGAGTTCCCACCA

IL, interleukin; TNF-α, tumor necrosis factor-α; Bcl-2, B-cell lymphoma-2; Bax, Bcl-2 associated X protein; LC3, microtubule-associated protein 1A/1B-light chain 3.

(Merck KGaA). Finally, the slices were observed by optical microscopy. Five random fields of views for each slice were analyzed. The ratios of brown stained areas vs. total areas were calculated using Image-Pro Plus software 6.0.

TUNEL assay. A TUNEL assay was performed according to the kit manufacturer's protocol. The prepared paraffin-embedded 3-μm liver sections were dewaxed in xylene for 10 min twice and dehydrated with ethanol. Then, 20 μg/ml DNase-free proteinase K was added at room temperature for 15 min. The TUNEL reaction mixture was added to the sections at 37˚C in a humidified atmosphere for 1 h, and the sections were observed by optical microscopy. The positive areas with dark brown nuclei were calculated using Image-Pro Plus software 6.0. Five random fields of views were examined for each section.

Primary hepatocyte isolation. Primary hepatocytes were isolated with a two-step perfusion method according to a previously described method (33,36-38). A total of 12 mice were anesthetized by intraperitoneal injection of 40 mg/kg 1.25% pentobarbital. After sterilization with 75% alcohol, the mice were laparotomized, and the hepatic portal vein was perfused with 10 ml pre-warmed D-Hanks buffer, then with 5 ml 0.02% type V collagenase solution. Then, the removed liver tissues were cut into small pieces and placed in collagenase V solution at 37˚C for 30 min. The cell suspensions were then filtered through two layers of gauze and centrifuged at 800 x g at room temperature for 5 min. RPMI-1640 culture medium (Thermo Fisher Scientific, Inc.) was added, then the cells were incubated at 5% CO_2 and 37˚C. The viability of the isolated hepatocytes was determined with Trypan blue exclusion. The cells were stained with 0.4% Trypan blue at room temperature for 3 min, and cell viability was counted using blood counting chamber. Dead cells are able to take in Trypan blue turn blue, whereas living cells cannot. The viability of the isolated hepatocytes exceeded 95%. Mouse death was confirmed by cervical dislocation.

Cell culture and CCK8 assay. The primary hepatocytes were cultured in RPMI-1640 culture medium with 10% fetal bovine serum (HyClone; GE Healthcare, Logan, UT, USA), 100 U/ml penicillin and 100 g/ml streptomycin (Gibco; Thermo Fisher Scientific, Inc.) in a humidified incubator at 37˚C under 5% CO_2. The apparent logarithmic phase cells were seeded at a density of $2x10^4$ cells/well in 96-well plates (100 μl of medium per well), and the Sal concentration was 10, 20, 40, 60, 80 or 100 μM (39,40). After 24 h, TNF-α was added to induce hepatocyte injuries at a concentration of 10 ng/ml (36). Cell viability was measured with the CCK8 assay, according to the manufacturer's protocol. The primary hepatocytes were divided into five groups: i) NC, no treatment; ii) Sal, treated with Sal diluted in ddH_2O at a concentration of 40 μM; iii) TNF-α, treated with TNF-α dissolved at a concentration of 10 ng/ml; iv) TNF-α + Sal, Sal (40 μM) was administered 24 h before TNF-α treatment; v) TNF-α + Sal + LY294002, Sal (40 μM) and LY294002 (40 μM) were administered 24 h before TNF-α treatment. At 24 h after TNF-α treatment, cells were collected for flow cytometry detection and western blot analysis as described above.

Flow cytometry analysis. The Annexin V-FITC apoptosis detection kit was purchased from BD Biosciences (San Jose, CA, USA). Following the different treatments the primary hepatocytes were collected and stained with FITC and propidium iodide according to the manufacturer's protocol. The results were analyzed using a flow cytometer (Beckman Coulter, Inc., Brea, CA, USA) and the data was analyzed using software FlowJo software version 10 (FlowJo LLC, Ashland, OR, USA).

Statistical analysis. Data are presented as the mean + standard deviation and experiments were repeated at least three times. The Student's t-test and one-way analysis of variance (followed by Tukey's post-hoc test) were used to analyze all results. GraphPad Prism 6 (GraphPad Software, Inc., La Jolla, CA, USA) was used for analysis. $P<0.05$ was considered to indicate a statistically significant difference.

Results

Sal does not affect liver function or the inflammatory response. To exclude any potential detrimental effects of Sal treatment, liver enzymes and hemotoxylin and eosin (H&E)-stained liver sections were examined after exposure to Sal at 20 mg/kg for 24 h. As indicated in Fig. 1A, serum ALT and AST levels did

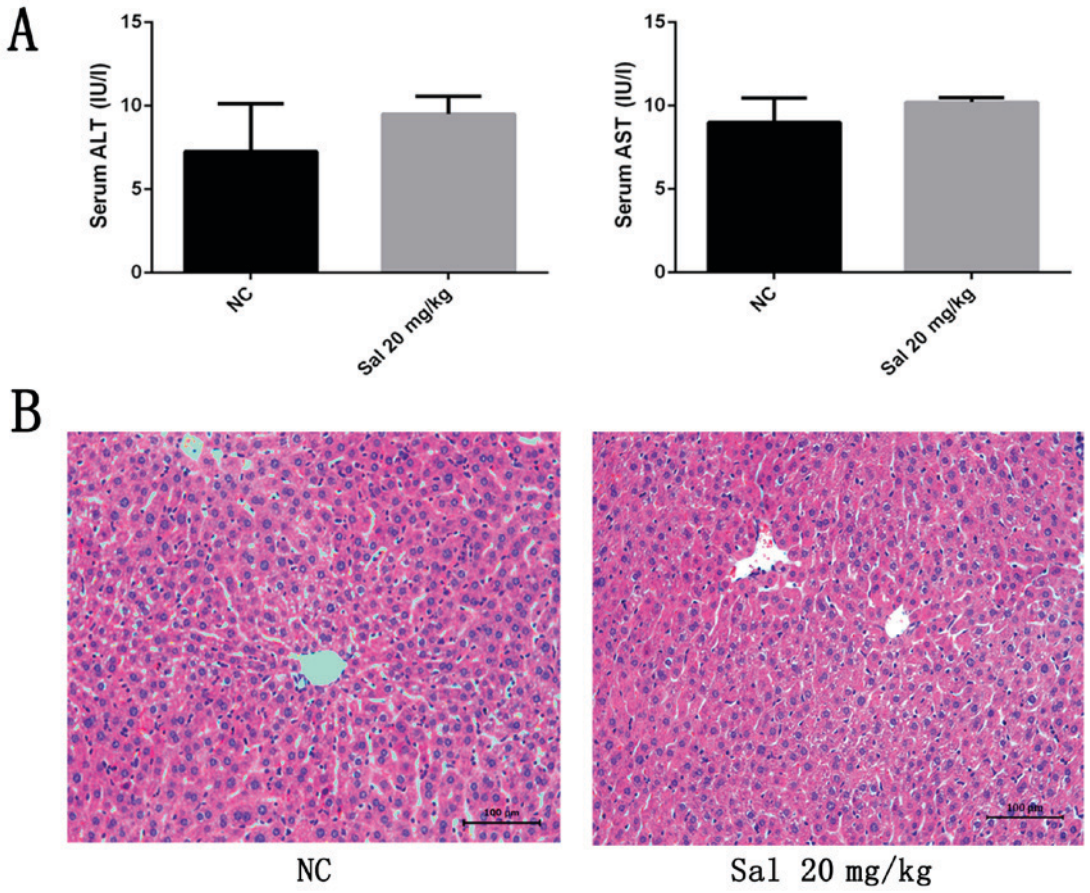

Figure 1. Effects of Sal on liver function and pathology of healthy mice. (A) Serum ALT and AST levels. Data are presented as the mean + standard deviation (n=6). (B) Representative hematoxylin and eosin-stained sections of the liver (original magnification, x200). NC, negative control; ALT, alanine aminotransferase; AST, aspartate aminotransferase; Sal, salidroside.

not differ between the Sal-treated and NC groups. As indicated in Fig. 1B, treatment with 20 mg/kg Sal did not cause obvious necrosis or inflammation in H&E-stained sections. These findings indicate that Sal has no adverse effect on liver function or the inflammatory response in mice.

Sal pretreatment attenuates liver injury induced by ConA in mice. To determine the effects of Sal pretreatment on ConA-induced liver injury, serum ALT and AST levels were measured and H&E staining was performed. The results indicated that ConA significantly increased serum ALT and AST levels compared with the control. However, Sal treatment at 10 or 20 mg/kg significantly decreased the levels of these liver enzymes compared with ConA treatment, and 20 mg/kg Sal exhibited a significantly stronger effect compared with 10 mg/kg Sal (Fig. 2A). As indicated in Fig. 2B, extensive areas of necrosis and an increased inflammatory response were observed in liver tissues treated with ConA alone, and these effects increased over time. However, Sal treatment attenuated these effects at the three time points, particularly in the 20 mg/kg Sal group. These histopathological changes were quantified using Image-Pro Plus software 6.0, and the differences between the four groups were statistically significant (Fig. 2C). In summary, these results indicate that pretreatment with Sal effectively reduces liver injury induced by ConA, and 20 mg/kg Sal has an increased protective effect compared with 10 mg/kg Sal.

Sal pretreatment reduces the production of IL-1β, IL-6 and TNF-α in ConA-induced liver injury. ConA may induce hepatitis, which not only results in inflammatory infiltration in liver tissues, but also increases the levels of pro-inflammatory cytokines in the serum, including IL-1β, IL-6 and TNF-α (13). Therefore, in the current study, the degree of inflammation was detected by measuring the serum levels of IL-6 and TNF-α, the mRNA and protein levels of pro-inflammatory cytokines in liver tissues, and the histochemical pro-inflammatory cytokine expression. The serum levels of IL-6 and TNF-α were significantly increased in the ConA group compared with the control. Out of the three detected time points, the serum IL-6 levels were highest at 2 h after ConA injection, while TNF-α levels were highest at 8 h after ConA injection (Fig. 3A). Sal pretreatment significantly reduced the serum levels of IL-6 and TNF-α compared with ConA treatment alone, particularly at 20 mg/kg Sal. The results of qPCR and western blot analyses were similar to those of ELISA regarding the mRNA and protein expression of IL-1β, IL-6 and TNF-α (Fig. 3B-D). In the majority of cases Sal (20 mg/kg) was more effective at reducing the expression of the inflammatory cytokines in liver tissues compared with Sal (10 mg/kg). However, as for TNF-α expression, the statistical analysis of western blot at 8 and 24 h revealed that Sal 10 mg/kg exhibited a stronger protective effect. These results may due to the possibility that Sal (at a higher dosage) may lead to the inhibition of

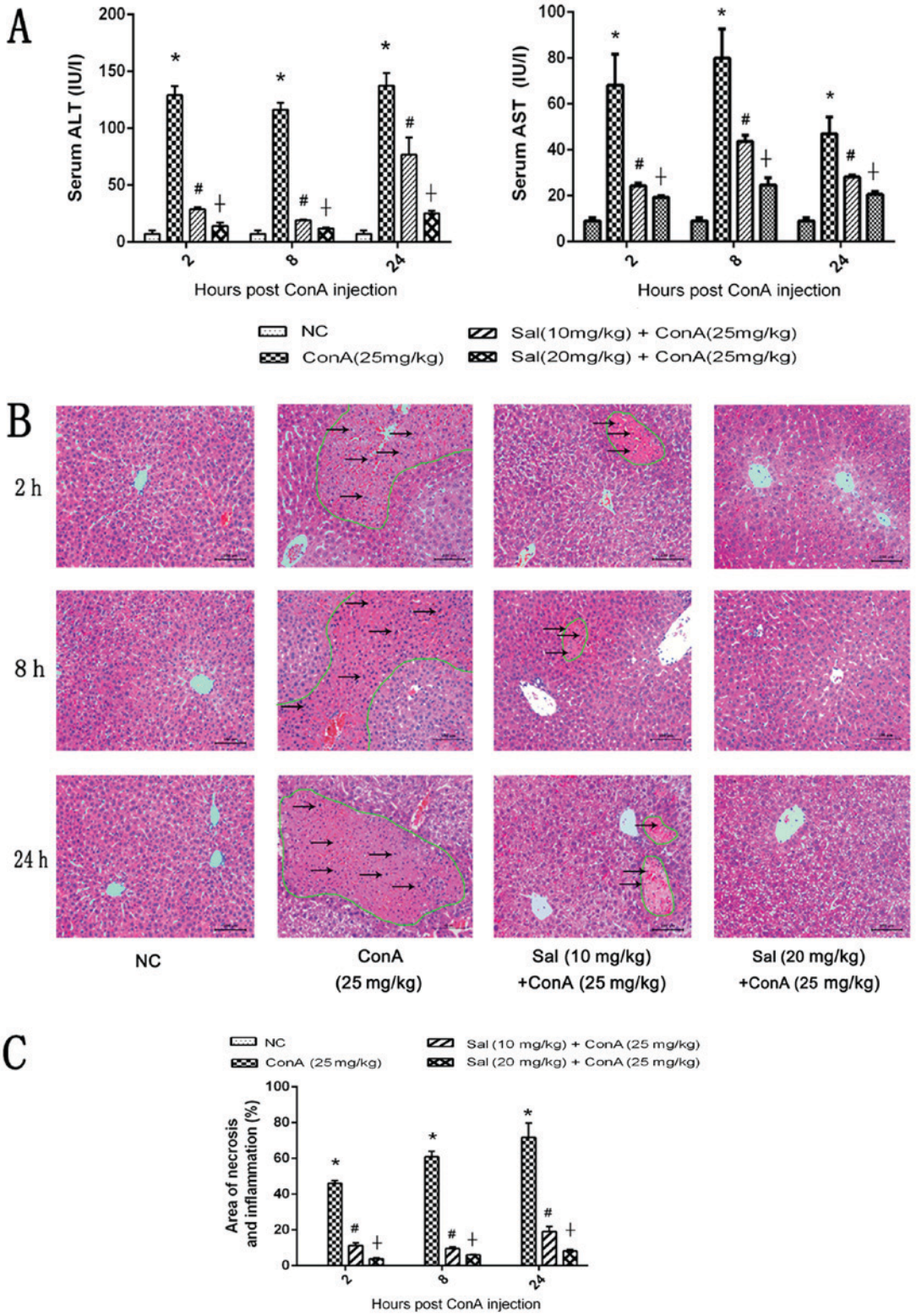

Figure 2. Effects of Sal on liver function and pathology of mice in ConA-induced liver injury. (A) Levels of serum ALT and AST. (B) H&E staining of liver sections (original magnification, x200). There were extensive areas of necrosis, which were eosinophilic and disorganized (circled by green lines), and an increased inflammatory response (indicated by black arrows) in liver tissues treated with ConA alone, and these effects increased over time. However, Sal treatment attenuated these effects at the three time points, indicated by the decreased areas of necrosis. (C) Necrotic and edema areas in H&E-stained sections were analyzed with Image-Pro Plus software 6.0. Data are presented as the mean + standard deviation (n=6). *P<0.05 vs. NC; #P<0.05 vs. ConA (25 mg/kg); †P<0.05 vs. Sal (10 mg/kg) + ConA (25 mg/kg). Sal, salidroside; ConA, concanavalin A; NC, negative control; H&E, hematoxylin and eosin; ALT, alanine aminotransferase; AST, aspartate aminotransferase.

apoptosis and autophagy of hepatocytes, therefore the injured but not dead cells induced an excessive secretion of TNF-α in liver tissues. Immunohistochemical staining was used to determine the expression of IL-6 and TNF-α (Fig. 3E), and

the results were consistent with those of ELISA, qPCR and western blot analyses. These results provided strong evidence that pretreatment with Sal may reduce the release of inflammatory cytokines, including IL-1β, IL-6 and TNF-α, in ConA-induced liver injury at the transcriptional and translational levels.

Sal pretreatment attenuates hepatocyte apoptosis in ConA-induced liver injury. B-cell lymphoma-2 (Bcl-2) is considered to be an anti-apoptotic protein, while Bcl-2-associated X protein (Bax), caspase-3 and caspase-9 are known to be markers of apoptosis (17). RT-qPCR and western blot analysis were performed to detect the expression of apoptosis markers at the mRNA and protein levels. As indicated in Fig. 4A-C, the relative expression of Bax, caspase-3 and caspase-9 was significantly enhanced at the three time points after ConA treatment compared with the control; however, this enhancement was significantly attenuated by pretreatment with Sal. Relative expression of Bcl-2 exhibited the opposite results. The results of immunohistochemical staining were consistent with those of qPCR and western blotting (Fig. 4D). Furthermore, a TUNEL assay was performed to investigate apoptosis levels in liver tissues. The positive areas, which represented apoptotic cells, were significantly larger in the ConA group compared with the NC group. However, in the Sal pretreated groups, the positive ratio was significantly decreased and 20 mg/kg Sal exhibited a larger effect compared with 10 mg/kg Sal (Fig. 4E). These results demonstrate that Sal may attenuate hepatocyte apoptosis in ConA-induced liver injury.

Sal pretreatment inhibits hepatocyte autophagy in ConA-induced liver injury. Beclin-1 and LC3 serve key functions in the process of autophagy (17). p62 is an ubiquitin-binding protein involved in autophagy that can be degraded in autophagosomes (41). RT-qPCR and western blot analyses indicated that ConA significantly upregulated beclin-1 and LC3 expression and significantly downregulated p62 expression compared with the control (Fig. 5A-C). However treatment with Sal reversed this effect, particularly Sal (20 mg/kg). There was an exception as Sal (10 mg/kg) had a better effect at inhibiting the ration of LC3 II/LC3 I at 8 and 24 h. This was consistent with the statistical analysis of the western blot analysis of TNF-α in Fig. 3D, where a higher TNF-α level may also lead to a higher level of hepatocytes injuries and autophagy. Immunohistochemical analysis revealed a significantly increased expression of beclin-1 and LC3 in the ConA group compared with the NC group (Fig. 5D). Treatment with Sal significantly downregulated the expression of beclin-1 and LC3 and Sal (20 mg/kg) was significantly more effective than Sal (10 mg/kg). (Fig. 5D). These results demonstrate that Sal inhibits autophagy in hepatocytes.

Sal activates the PI3K/Akt signaling pathway in ConA-induced liver injury. To determine whether the protective effect of Sal on ConA-induced liver injury is mediated by the PI3K/Akt signaling pathway, the protein levels of PI3K, Akt and phosphorylated (p-)Akt were detected. The results indicated that ConA injection downregulated PI3K and p-Akt/Akt at the three time points tested compared with the levels in the NC group. However, Sal pretreatment suppressed the decreasing effect significantly at 2 and 24 h (Fig. 6A). Immunohistochemistry of PI3K and p-Akt also indicated a significant decrease in protein levels in the ConA group compared with the control, and a significant increase in the Sal pretreated groups (Fig. 6B). In summary, these results indicate that Sal pretreatment may activate the PI3K/Akt signaling pathway in ConA-induced liver injury.

Sal pretreatment ameliorates liver injury in ConA-induced liver injury, at least in part through the PI3K/Akt signaling pathway. LY294002, a specific inhibitor of PI3K, was used to verify whether the protective effect of Sal was associated with PI3K. Levels of serum liver enzymes and the mRNA and/or protein expression of TNF-α, IL-6, Bcl-2, Bax, beclin-1, LC3 and p-Akt were detected with or without LY294002 treatment. As indicated in Fig. 7, the protective effective of Sal was significantly reversed by LY294002, with an increase of liver enzymes, an increase of TNF-α, IL-6, Bax, beclin-1 and LC3 mRNA and protein levels, a decrease of Bcl-2 mRNA and protein levels and a decrease of p-Akt protein levels. These results suggest that Sal could activate the PI3K/Akt signaling pathway in ConA-induced liver injury. In addition, these results indicate that the inflammatory response, apoptosis and autophagy processes, which lead to liver injuries in this model, are associated with the PI3K/Akt pathway.

Sal increases cell viability and reduces cell apoptosis induced by TNF-α in vitro. The hepatocyte viability was measured by CCK8 assay. In the Sal (0 μM) group where the cells were treated with TNF-α alone the viability of the cells was reduced to 21.55±1.52% (data not shown). When the cells were treated with Sal, their viability was then gradually enhanced (Fig. 8A). The results indicated that hepatocyte viability was injured by TNF-α treatment (data not shown). However, Sal pretreatment could enhance hepatocyte viability in a dose-dependent manner (Fig. 8A). The half maximal inhibitory concentration (IC_{50}) of Sal was 37.61 μM. This indicated that Sal protected the primary hepatocytes from inflammatory damage induced by TNF-α. Then, 40 μM Sal was used for subsequent treatment. The flow cytometry and western blot results of Bcl-2 and Bax indicated that TNF-α treatment could significantly induce apoptosis in primary hepatocytes (Fig. 8B-E). However, pretreatment with Sal significantly reduced the induction of apoptosis (Fig. 8B). LY294002 was used to detect whether the PI3K/Akt signaling pathway was activated in hepatocytes by western blot analysis. The results revealed that if cells were treated with Sal alone, the tested protein expression did not significantly change. This confirmed the safety of Sal *in vitro*. In the TNF-α group, the protein expression of p-Akt and Bcl-2 were significantly reduced compared with the NC group, while the Bax, Beclin-1 and LC3 II/LC3 I levels were significantly enhanced (Fig. 8E). However, when the cells were treated with a combination of TNF-α and Sal the results were reversed, which indicated that Sal may inhibit the apoptosis and autophagy process *in vitro*. When the cells were co-treated with Sal and LY294002 the protective effects of Sal were reversed. This suggested that

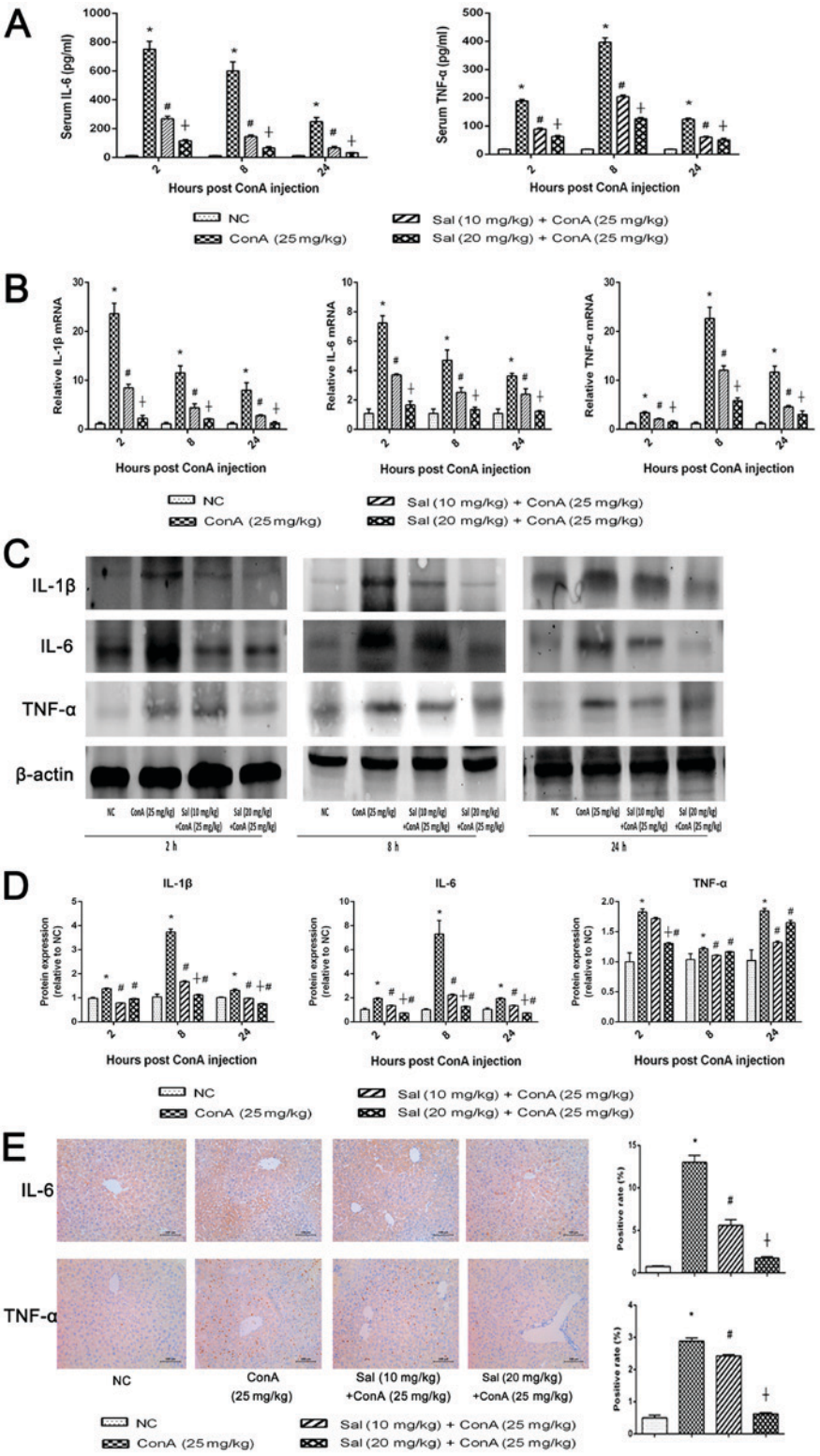

Figure 3. Sal pretreatment inhibits the release of IL-1β, IL-6 and TNF-α in ConA-induced liver injury. (A) Serum IL-6 and TNF-α levels were measured using ELISA kits at 2, 8 and 24 h after ConA injection in mice. (B) Relative mRNA levels of IL-1β, IL-6 and TNF-α were evaluated in each group by reverse transcription-quantitative polymerase chain reaction. (C and D) Protein expression of IL-1β, IL-6 and TNF-α was detected by western blot analysis. (E) Immunohistochemistry was used to detect IL-6 and TNF-α expression in liver tissues (original magnification, x200). The ratio of brown area to total area was analyzed with Image-Pro Plus software 6.0. Data are presented as the mean + standard deviation (n=6). *P<0.05 vs. NC; #P<0.05 vs. ConA (25 mg/kg); ‡P<0.05 vs. Sal (10 mg/kg) + ConA (25 mg/kg). Sal, salidroside; ConA, concanavalin A; NC, negative control; IL, interleukin; TNF-α, tumor necrosis factor-α.

the PI3K/Akt signaling pathway was activated by TNF-α and the apoptosis and autophagy levels were regulated through the PI3K/Akt signaling pathway (Fig. 8D and E).

Discussion

AIH was first reported by Jan Waldeöm in 1950 (3). AIH may

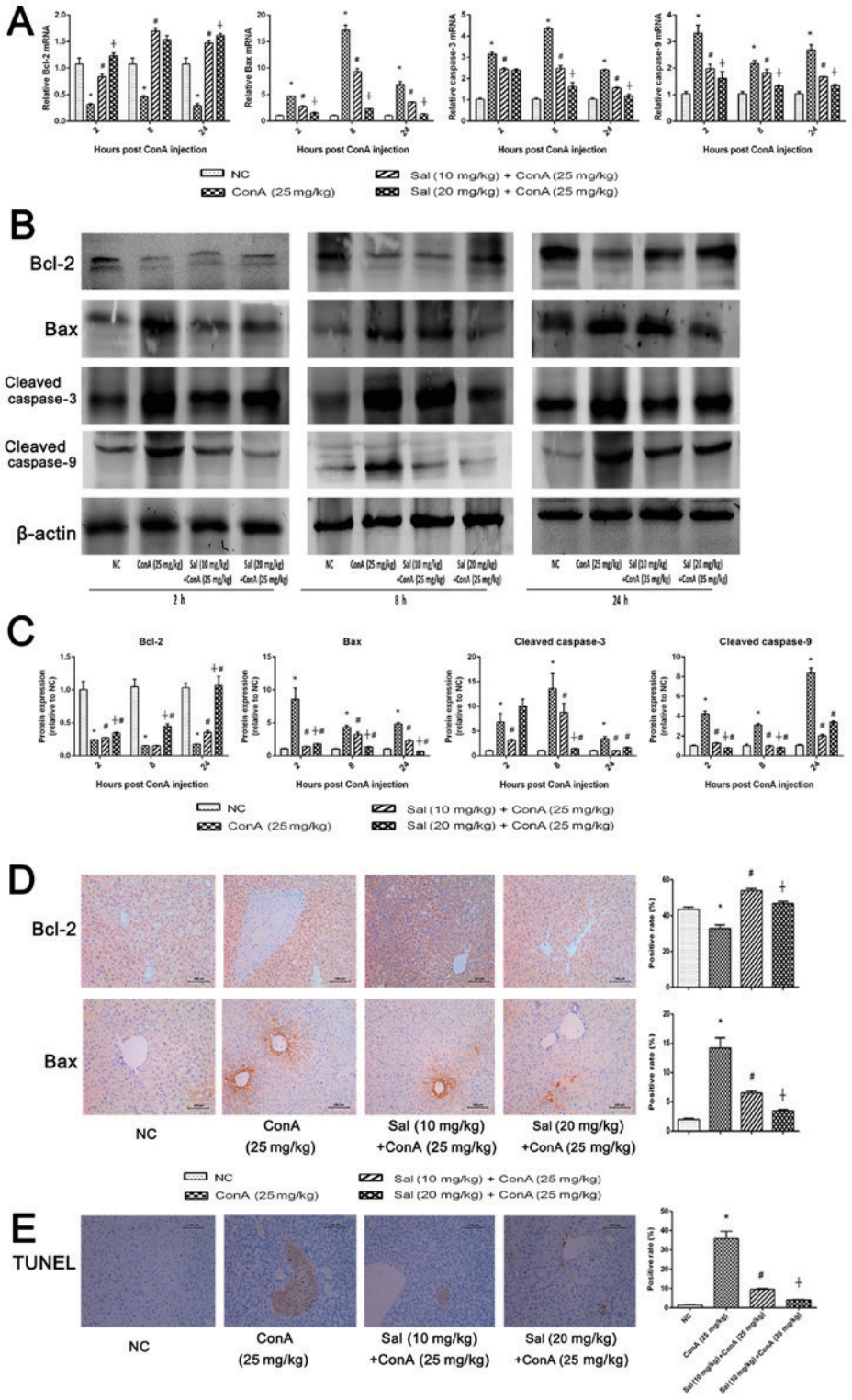

Figure 4. Sal pretreatment downregulates apoptosis in ConA-induced liver injury. (A) Relative mRNA levels of Bcl-2, Bax, caspase-3 and caspase-9. (B and C) Protein expression of Bcl-2, Bax, caspase-3 and caspase-9. (D) Immunohistochemistry was used to detect Bcl-2 and Bax (original magnification, x200). The ratio of brown area to total area was analyzed with Image-Pro Plus software 6.0. (E) TUNEL staining indicated apoptotic cells in the four groups at 8 h after ConA injection (original magnification, x200). The percentage of TUNEL-positive cells was determined by Image-Pro Plus software 6.0. Data are presented as the mean + standard deviation (n=6). *P<0.05 vs. NC; #P<0.05 vs. ConA (25 mg/kg); †P<0.05 vs. Sal (10 mg/kg) + ConA (25 mg/kg). Sal, salidroside; ConA, concanavalin A; NC, negative control; Bcl-2, B-cell lymphoma-2; Bax, Bcl-2-associated X protein.

progress to end-stage liver disease, including liver cirrhosis or even hepatocellular carcinoma (42). Currently, immunosuppressive treatment is primarily used in the clinic (3). ConA is used as a suitable animal model to establish AIH *in vivo*, providing opportunities for researchers to investigate the mechanism and treatment of AIH (36,43,44).

Wu *et al* (22) reported that Sal exerts protective effects against acetaminophen-induced liver toxicity in mice. Sal was

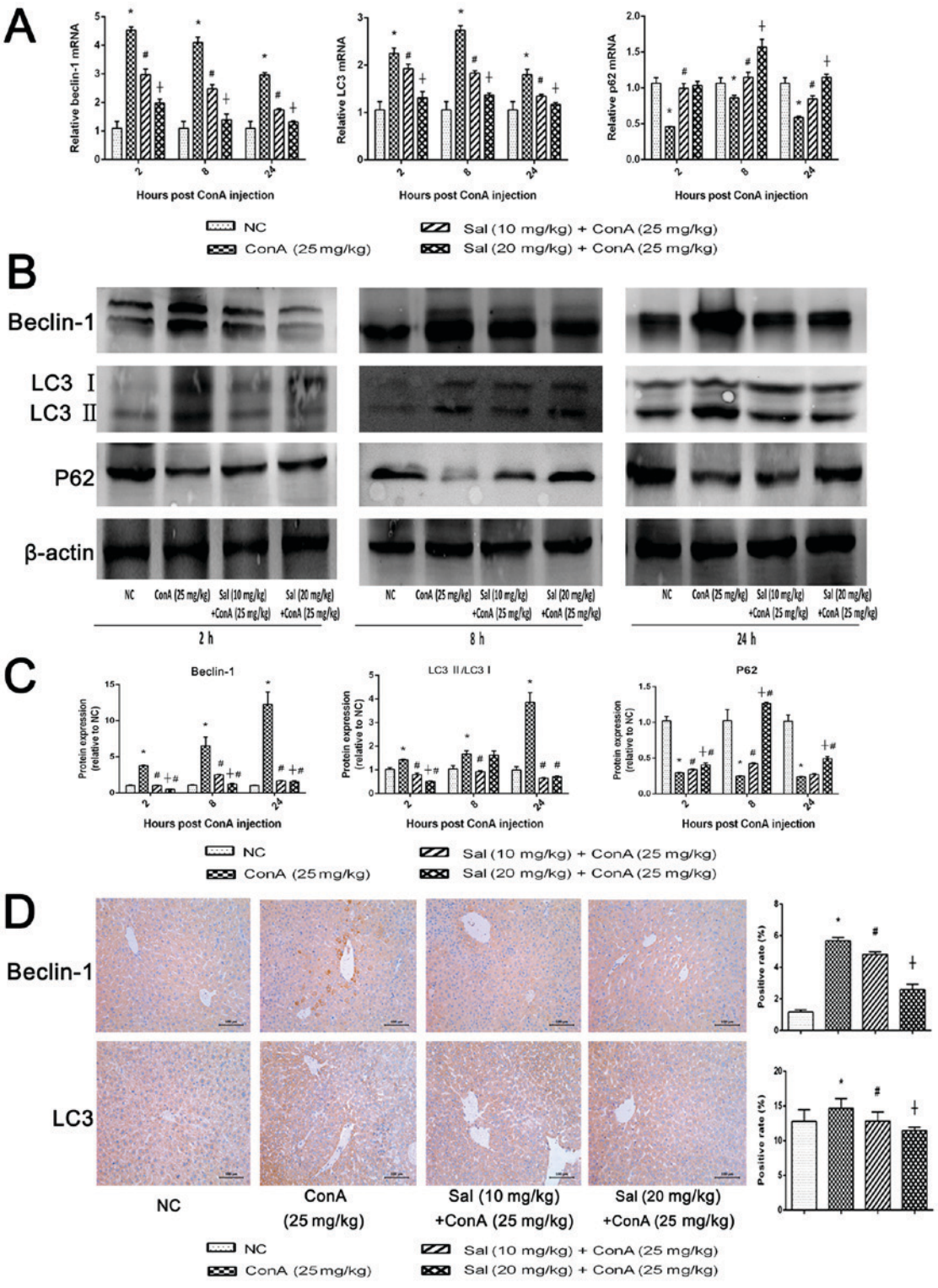

Figure 5. Sal pretreatment attenuates hepatocyte autophagy in ConA-induced liver injury. (A) Relative mRNA levels of beclin-1, LC3 and p62. (B and C) Protein expression of beclin-1, LC3 and p62. (D) Immunohistochemistry was used to detect beclin-1 and LC3 levels in liver tissues (original magnification, x200). The ratio of brown area to total area was analyzed with Image-Pro Plus software 6.0. Data are presented as the mean + standard deviation (n=6). *P<0.05 vs. NC; $^{\#}$P<0.05 vs. ConA (25 mg/kg); †P<0.05 vs. Sal (10 mg/kg) + ConA (25 mg/kg). Sal, salidroside; ConA, concanavalin A; NC, negative control; LC3, microtubule-associated protein 1A/1B-light chain 3.

also demonstrated to alleviate oxidative damage in the livers of rats with non-alcoholic steatohepatitis (27). Our previous study indicated that Sal could reduce hepatic ischemia reperfusion injury (32). These findings suggest that Sal exerts beneficial effects on liver function.

In the present study, it was identified that Sal functioned as an anti-inflammatory agent to prevent ConA-induced liver injury in mice. Inflammation is the central process of ConA-induced liver injury. After intravenous injection, ConA accumulates specifically in the liver, binding to the

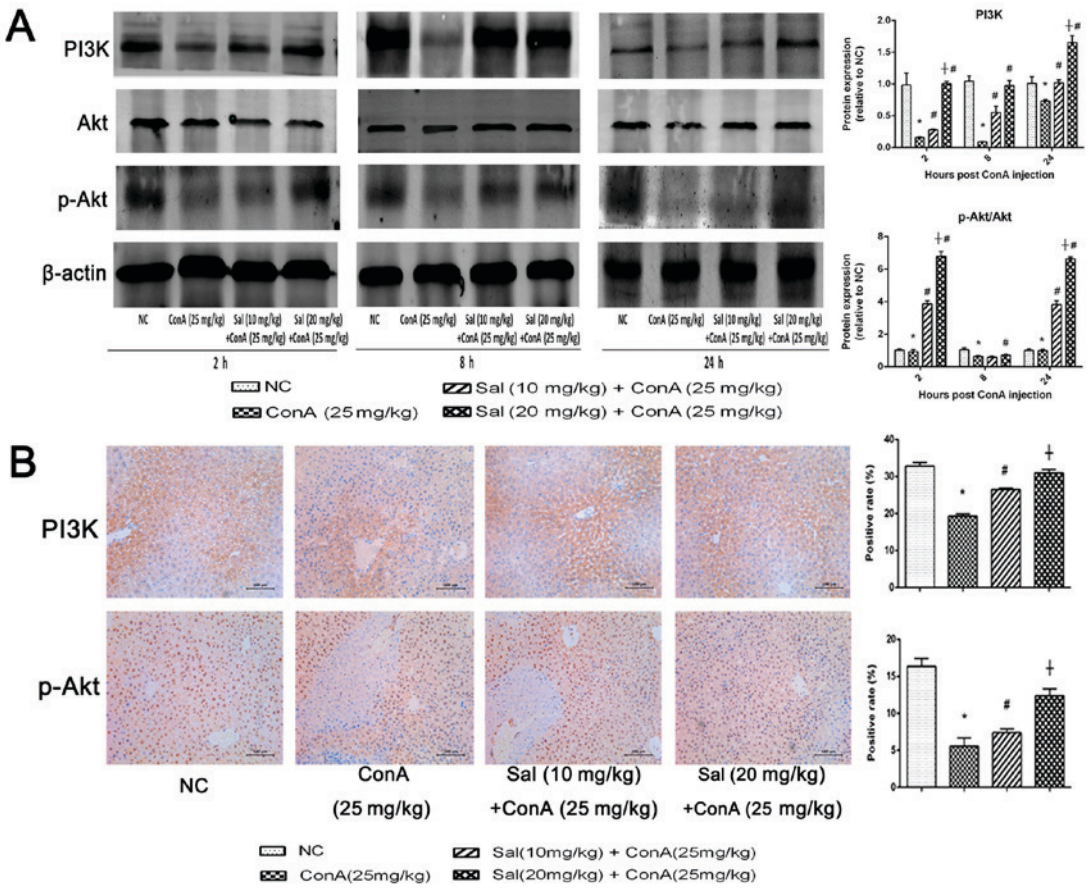

Figure 6. Sal activates the PI3K/Akt signaling pathway in ConA-induced liver injury. (A) Protein expression of PI3K, Akt and p-Akt. (B) Immunohistochemistry was used to detect PI3K and p-Akt levels in liver tissues (original magnification, x200). The ratio of brown area to total area was analyzed with Image-Pro Plus software 6.0. Data are presented as the mean + standard deviation (n=6). *P<0.05 vs. NC; #P<0.05 vs. ConA (25 mg/kg); †P<0.05 vs. Sal (10 mg/kg) + ConA (25 mg/kg). Sal, salidroside; ConA, concanavalin A; NC, negative control; PI3K, phosphoinositide 3-kinase; p-, phosphorylated.

mannose-rich glycoproteins on liver sinusoidal endothelial cells (5,6,45). This leads to the activation of T cells, particularly $CD4^+$ T cells. Finally, T cells secrete a series of cytokines, including IL-1β, IL-6, TNF-α, IFN-γ and IL-2. When inflammation occurs, it results in liver injury and the elevation of aminotransferase levels in the serum (5,6,19,45). In the present study, the results indicated that pretreatment with Sal suppressed the release of IL-1β, IL-6 and TNF-α in the serum and in liver tissue. Therefore, the inflammatory reaction is inhibited by Sal to protect liver tissues from ConA-induced liver injury.

A number of studies have demonstrated that Sal may activate the PI3K/Akt pathway to protect cardiomyocytes, hepatocytes and brain function, and protect against colorectal cancer (21,23,46,47). Based on these findings, it was examined whether the effects of Sal pretreatment were mediated by the regulation of PI3K/Akt signaling in the current model. LY294002 is a potent and reversible inhibitor of PI3K, which competes for the ATP binding site of PI3K, resulting in cell cycle arrest, induction of apoptosis and negative feedback of the inflammatory response (34,48). The current results indicated that the protein level of p-Akt was decreased in ConA-treated groups, whereas Sal reversed this effect. However, if LY294002 was used, the protective effect of Sal was reversed again. Hence, it was concluded that Sal acts as a protective factor in ConA-induced liver injury by activating the PI3K/Akt pathway.

The PI3K/Akt pathway is widespread in cells and serves key functions in cell growth, proliferation, apoptosis and autophagy (49-51). Following activation, PI3K further activates Akt, leading to its phosphorylation and translocation from the cytoplasm to the cell membrane. The activation of p-Akt causes a series of changes in cytokines associated with apoptosis. Firstly, p-Akt phosphorylates Bcl-2-associated death promoter (Bad), a pro-apoptotic Bcl-2 family member, inhibiting the interaction between Bad and Bcl-2. The release of Bcl-2 has an anti-apoptotic effect, leading to the inhibition of its proteolytic activity (49). Secondly, p-Akt phosphorylates Bax, which translocates to the mitochondrion and induces the release of cytochrome c and the activation of caspases (52). Bax is inactivated by phosphorylation, leading to the inhibition of apoptosis. Thirdly, p-Akt also phosphorylates caspase-9 at Ser196, activating the conversion of procaspase-3 into caspase-3 causing a conformational change and leading to the inhibition of its proteolytic activity. This results in apoptosis (Fig. 9) (53).

In the current study, the expression of apoptosis-associated proteins was evaluated in liver tissues, including Bcl-2, Bax, caspase-3 and caspase-9. The results indicated that Sal upregulated the expression of Bcl-2 and downregulated the expression of Bax, caspase-3 and caspase-9. These results strongly support the hypothesis that Sal suppresses apoptosis in ConA-induced liver injury by activating the PI3K/Akt pathway.

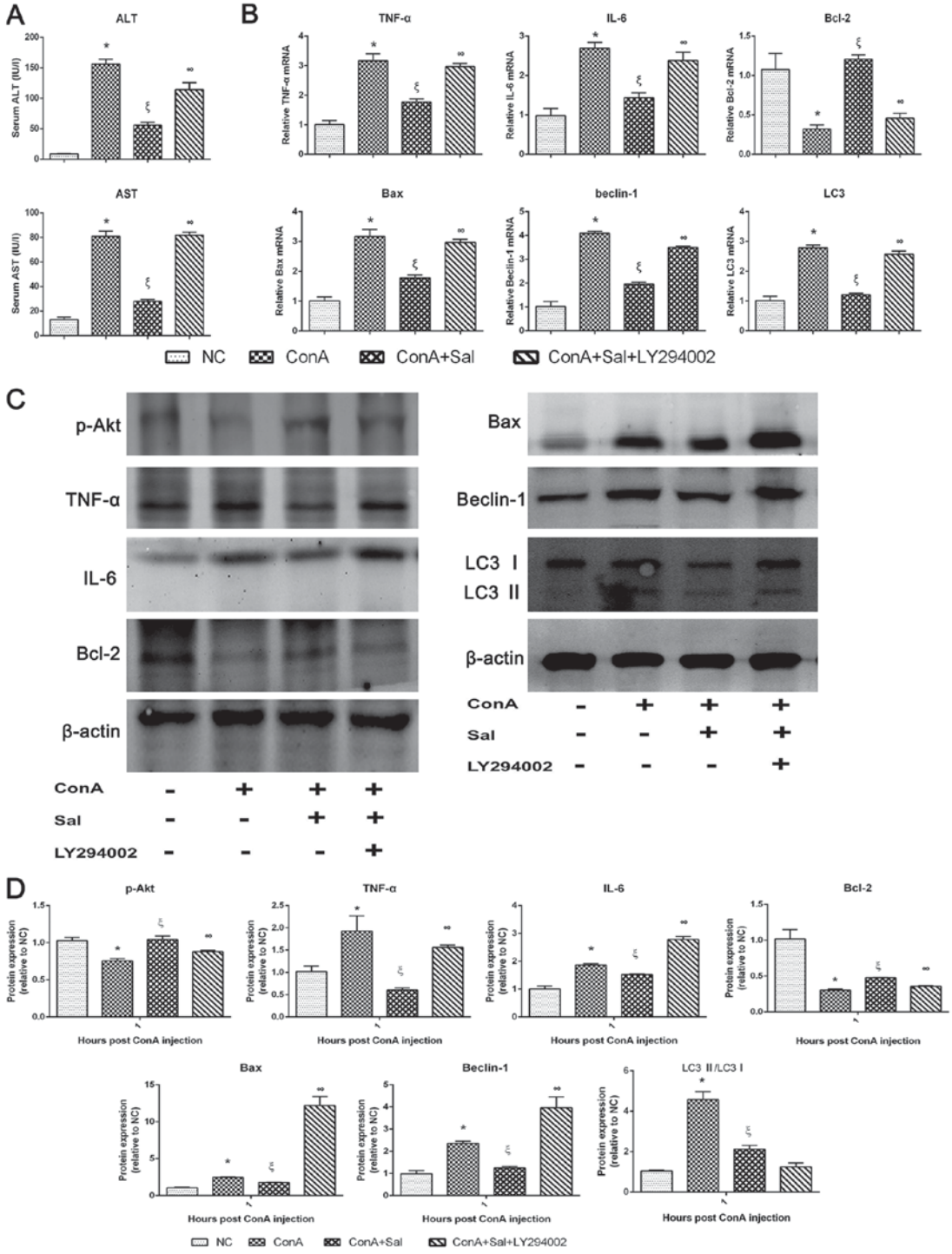

Figure 7. Protective effects of Sal on ConA-induced liver injury may be reversed by LY294002, a PI3K inhibitor. (A) Serum liver enzyme levels. (B) Relative mRNA levels of TNF-α, IL-6, Bcl-2, Bax, beclin-1 and LC3. (C and D) Protein expression of p-Akt, TNF-α, IL-6, Bcl-2, Bax, beclin-1, LC3 and β-actin. β-actin was used as the internal control. Data are presented as the mean + standard deviation (n=6). *P<0.05 vs. NC; §P<0.05 vs. ConA; ∞P<0.05 vs. ConA + Sal. Sal, salidroside; ConA, concanavalin A; NC, negative control; ALT, alanine aminotransferase; AST, aspartate aminotransferase; IL, interleukin; TNF-α, tumor necrosis factor-α; Bcl-2, B-cell lymphoma-2; Bax, Bcl-2-associated X protein; LC3, microtubule-associated protein 1A/1B-light chain 3; p-, phosphorylated.

The PI3K/Akt pathway serves a function in the regulation of autophagy (54). Autophagy was first described as a process by which cells digest organelles and recycle their components in 1963 (17,55). However, accumulating evidence suggests that autophagy also has a cytoprotective role under physiologically relevant conditions (12). The Japanese scientist Ohsumi Yoshinori won the Nobel Prize in 2016 for his contribution to elucidating the mechanism of autophagy. Beclin-1, the mammalian ortholog of the yeast protein autophagy-related gene-6, interacts with PI3K class III, also known as vesicular protein sorting 34 (VPS34), and serves a critical function in the nucleation process of autophagy (17). LC3 is widely used as a marker for monitoring the autophagy process. LC3 I exists in the cytosol, whereas LC3 II is conjugated to the

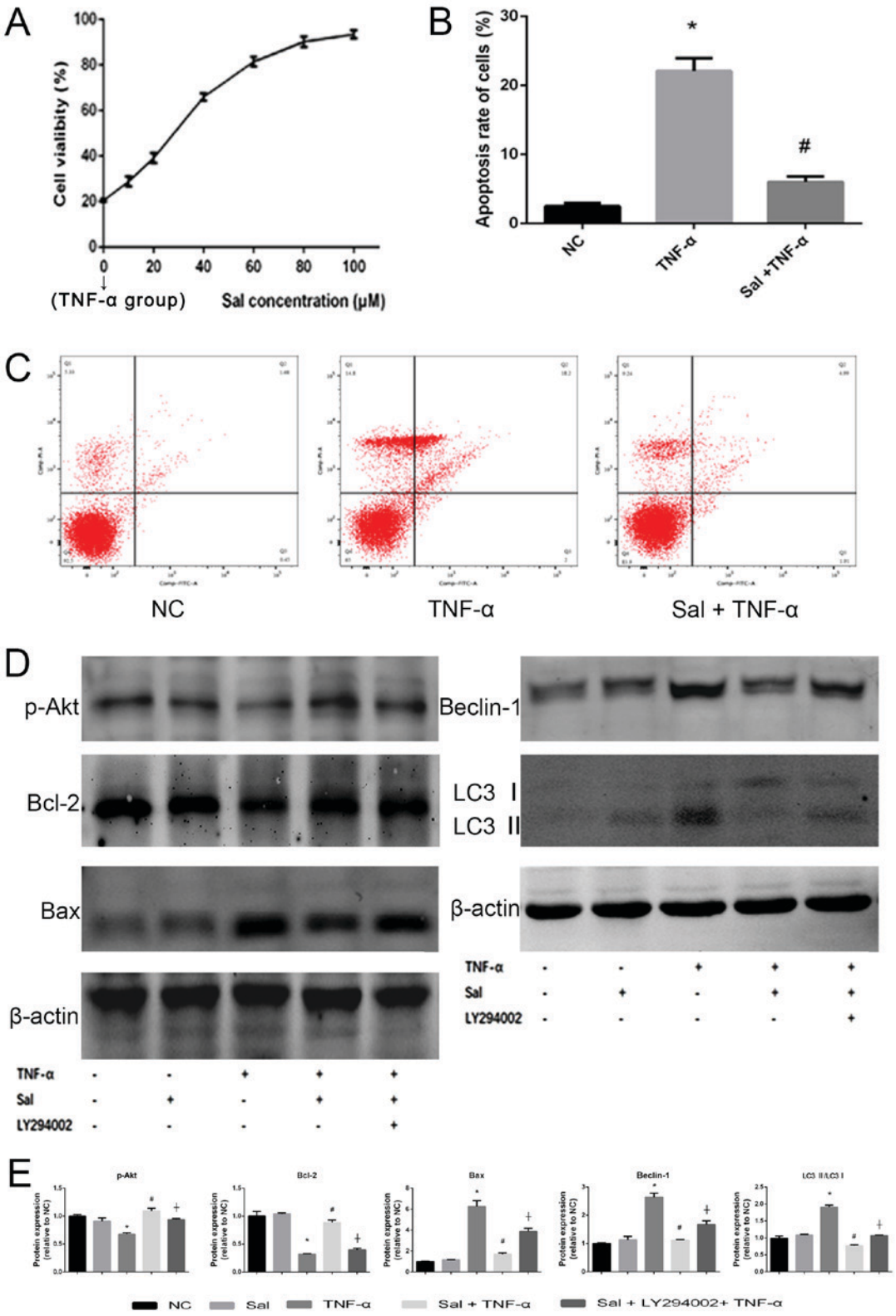

Figure 8. Sal increases primary hepatocyte viability and reduces apoptosis induced by TNF-α *in vitro*. (A) Primary hepatocyte viability was evaluated using a CCK8 assay. The IC_{50} of Sal was 37.61 μM. (B and C) Apoptosis rate of hepatocytes was detected by flow cytometry. (D and E) Protein expression of p-Akt, Bcl-2, Bax, beclin-1 and LC3 was measured by western blot analysis. β-actin was used as the internal control. Data are presented as the mean + standard deviation (n=3). *P<0.05 vs. NC; $^{\#}$P<0.05 vs. TNF-α; †P<0.05 vs. Sal + TNF-α. Sal, salidroside; ConA, concanavalin A; NC, negative control; TNF-α, tumor necrosis factor-α; Bcl-2, B-cell lymphoma-2; Bax, Bcl-2-associated X protein; LC3, microtubule-associated protein 1A/1B-light chain 3; p-, phosphorylated.

autophagosomal membrane and serves a key function in the membrane extension of autophagosomes and the eventual closure of the vesicle (9). Therefore, the LC3 II/LC3 I ratio is used as an index to evaluate the degree of autophagy. In addition, p62 is an ubiquitin-binding protein involved in autophagy that is selectively degraded in autophagosomes (41). Overall,

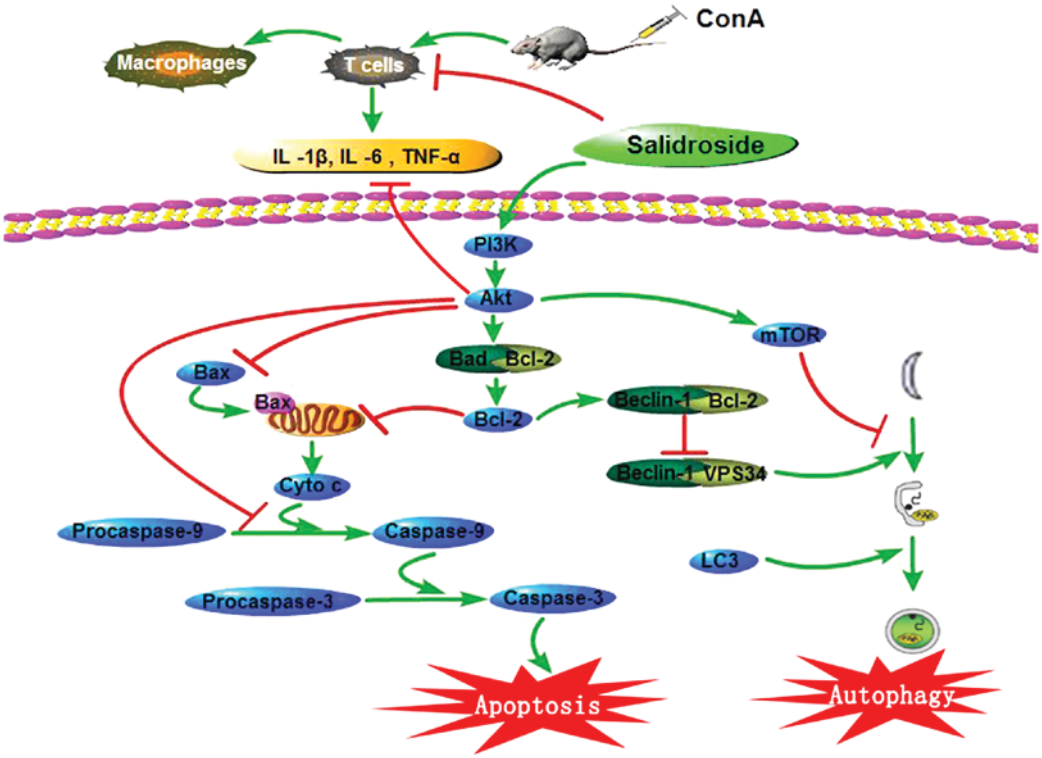

Figure 9. Sal ameliorates apoptosis and autophagy via activating the PI3K/Akt pathway in ConA-induced liver injury. In ConA-induced liver injury, the levels of IL-1β, IL-6 and TNF-α increase in the serum and liver tissues. Sal pretreatment reduces the production of these pro-inflammatory cytokines to relieve liver injury. Furthermore, Sal may activate the PI3K/Akt pathway to ameliorate liver injury. Following PI3K/Akt activation, Bad and Bax are phosphorylated and deactivated, and Bcl-2 is released from Bad, leading to the inhibition of apoptosis. Akt could also inhibit the production of caspase-9 to alleviate apoptosis. Released Bcl-2 conjugates with beclin-1 to form the Bcl-2/ beclin-1 complex, interfering with the interaction between beclin-1 and VPS34, inhibiting the autophagy process. Thus, Sal successfully decreases liver injury in ConA-induced liver injury in mice. Sal, salidroside; ConA, concanavalin A; Bcl-2, B-cell lymphoma-2; Bax, Bcl-2-associated X protein; Bcl-2-associated death promoter; LC3, microtubule-associated protein 1A/1B-light chain 3; IL, interleukin; TNF-α, tumor necrosis factor-α; PI3K, phosphoinositide 3-kinase; mTOR, mechanistic target of rapamycin; VPS34, vesicular protein sorting 34.

the levels of beclin-1 and the LC3 II/LC3 I ratio increase, while the level of p62 decreases, when autophagy is activated.

Autophagy is regulated by two pathways. The first pathway is mediated by Bcl-2, which acts on the beclin-1/VPS34 connection and regulates both apoptosis and autophagy. Bcl-2 interacts with beclin-1 under normal conditions, forming the Bcl-2/beclin-1 complex, which disrupts the interaction between beclin-1 and VPS34 and inhibits autophagy (17,41,56). However, under conditions of stress, such as the toxicity from ConA, the Bcl-2/beclin-1 complex is disrupted and autophagy is enhanced. The other pathway is the mechanistic target of rapamycin pathway, which is regulated by PI3K/Akt, mitogen-activated protein kinase/extracellular signal-regulated kinase and tuberous sclerosis protein 1/2, among others (10,12).

Previous studies have indicated that the autophagy process is enhanced in ConA-induced liver injury models (10-12,57). The results of the present study were consistent with previous findings. Furthermore, Sal pretreatment decreased the levels of beclin-1 and the LC3 II/LC3 I ratio and increased the level of p62. These findings indicate that Sal may relieve ConA-induced liver injury by regulating autophagy, possibly through the PI3K/Akt pathway.

Certain traditional Chinese preparations that contain Sal have been used in traditional Chinese medicine to improve cardiovascular disorders and chronic cerebral circulatory insufficiency (58). This suggests that it is possible to develop an efficient and stable Sal agent as a functional food to decrease the occurrence of AIH. This could be used clinically for the treatment of AIH, and potentially for other liver diseases. Sal also inhibits the proliferation of hepatocellular carcinoma cells *in vitro* (25). Since hepatitis, liver cirrhosis and hepatocellular carcinoma are closely connected, Sal may have potential uses as an anticancer agent as well.

It should be noted that the present study had several limitations. First, the mechanisms involved in ConA-induced liver injury are complex. Further research is required to elucidate the exact mechanism of ConA-induced liver injury. Second, the present study was performed in mice, and additional studies are required to examine the protective effects of Sal on liver injury in human beings.

In conclusion, the present study demonstrated that Sal is a safe agent for the treatment of liver injury in mice. It was identified that Sal may alleviate liver injury induced by ConA through two mechanisms. Firstly, Sal suppressed the inflammatory reaction in serum and liver tissues. Secondly, Sal activated the PI3K/Akt signaling pathway, inhibiting apoptosis and autophagy *in vivo* and *in vitro*. These results indicate that Sal may be a potential therapeutic agent for AIH.

Acknowledgements

Not applicable.

Funding

This study was supported by the National Natural Science Foundation of China (grant nos. 81670472, 81700502 and 81500466).

Availability of data and materials

The datasets generated and/or analyzed during the current study are available from the corresponding author on reasonable request.

Authors' contributions

JF, PN, XF, KC and CG designed the research. JF, LW, TL, JL, SL and SX performed the experiments. JF, WW, XL, QY, NL, LX, FW, WD and YX contributed to the collection and analysis of data. KC, YX, XF and CG were responsible for the revision of the manuscript. JF and CG supervised and coordinated the study.

Ethics approval and consent to participate

The study was approved by the Animal Care and Use Committee of Tongji University (Shanghai, China) and was performed in accordance with the National Institutes of Health Guide for the Care and Use of Laboratory Animals and the ARRIVE guidelines.

Consent for publication

Not applicable.

Competing interests

The authors declare that they have no competing interests.

References

1. Than NN, Jeffery HC and Oo YH: Autoimmune hepatitis: Progress from global immunosuppression to personalised regulatory T cell therapy. Can J Gastroenterol Hepatol 2016: 7181685, 2016.
2. Liberal R, Grant CR, Mieli-Vergani G and Vergani D: Autoimmune hepatitis: A comprehensive review. J Autoimmun 41: 126-139, 2013.
3. Heneghan MA, Yeoman AD, Verma S, Smith AD and Longhi MS: Autoimmune hepatitis. Lancet 382: 1433-1444, 2013.
4. Liberal R, Grant CR, Longhi MS, Mieli-Vergani G and Vergani D: Diagnostic criteria of autoimmune hepatitis. Autoimmun Rev 13: 435-440, 2014.
5. Tiegs G, Hentschel J and Wendel A: A T cell-dependent experimental liver injury in mice inducible by concanavalin A. J Clin Invest 90: 196-203, 1992.
6. Heymann F, Hamesch K, Weiskirchen R and Tacke F: The concanavalin A model of acute hepatitis in mice. Lab Anim 49 (1 Suppl): S12-S20, 2015.
7. Bies C, Lehr CM and Woodley JF: Lectin-mediated drug targeting: History and applications. Adv Drug Deliv Rev 56: 425-435, 2004.
8. Varthaman A, Khallou-Laschet J, Clement M, Fornasa G, Kim HJ, Gaston AT, Dussiot M, Caligiuri G, Herbelin A, Kaveri S, *et al*: Control of T cell reactivation by regulatory Qa-1-restricted CD8+ T cells. J Immunol 184: 6585-6591, 2010.
9. Yin XM, Ding WX and Gao W: Autophagy in the liver. Hepatology 47: 1773-1785, 2008.
10. Mao Y, Wang J, Yu F, Cheng J, Li H, Guo C and Fan X: Ghrelin reduces liver impairment in a model of concanavalin A-induced acute hepatitis in mice. Drug Des Devel Ther 9: 5385-5396, 2015.
11. Li S, Xia Y, Chen K, Li J, Liu T, Wang F, Lu J, Zhou Y and Guo C: Epigallocatechin-3-gallate attenuates apoptosis and autophagy in concanavalin A-induced hepatitis by inhibiting BNIP3. Drug Des Devel Ther 10: 631-647, 2016.
12. Liu T, Xia Y, Li J, Li S, Feng J, Wu L, Zhang R, Xu S, Cheng K, Zhou Y, *et al*: Shikonin attenuates concanavalin A-induced acute liver injury in mice via inhibition of the JNK pathway. Mediators Inflamm 2016: 2748367, 2016.
13. Li J, Chen K, Li S, Liu T, Wang F, Xia Y, Lu J, Zhou Y and Guo C: Pretreatment with fucoidan from fucus vesiculosus protected against ConA-induced acute liver injury by inhibiting both intrinsic and extrinsic apoptosis. PLoS One 11: e0152570, 2016.
14. Gantner F, Leist M, Lohse AW, Germann PG and Tiegs G: Concanavalin A-induced T-cell-mediated hepatic injury in mice: The role of tumor necrosis factor. Hepatology 21: 190-198, 1995.
15. Czaja AJ: Targeting apoptosis in autoimmune hepatitis. Dig Dis Sci 59: 2890-2904, 2014.
16. Portt L, Norman G, Clapp C, Greenwood M and Greenwood MT: Anti-apoptosis and cell survival: A review. Biochim Biophys Acta 1813: 238-259, 2011.
17. Gordy C and He YW: The crosstalk between autophagy and apoptosis: Where does this lead? Protein Cell 3: 17-27, 2012.
18. Pyo JO, Jang MH, Kwon YK, Lee HJ, Jun JI, Woo HN, Cho DH, Choi B, Lee H, Kim JH, *et al*: Essential roles of Atg5 and FADD in autophagic cell death: Dissection of autophagic cell death into vacuole formation and cell death. J Biol Chem 280: 20722-20729, 2005.
19. Hu B, Zou Y, Liu S, Wang J, Zhu J, Li J, Bo L and Deng X: Salidroside attenuates concanavalin A-induced hepatitis via modulating cytokines secretion and lymphocyte migration in mice. Mediators Inflamm 2014: 314081, 2014.
20. Palmeri A, Mammana L, Tropea MR, Gulisano W and Puzzo D: Salidroside, a bioactive compound of rhodiola rosea, ameliorates memory and emotional behavior in adult mice. J Alzheimers Dis 52: 65-75, 2016.
21. Zou H, Liu X, Han T, Hu D, Wang Y, Yuan Y, Gu J, Bian J, Zhu J and Liu ZP: Salidroside protects against cadmium-induced hepatotoxicity in rats via GJIC and MAPK pathways. PLoS One 10: e0129788, 2015.
22. Wu YL, Piao DM, Han XH and Nan JX: Protective effects of salidroside against acetaminophen-induced toxicity in mice. Biol Pharm Bull 31: 1523-1529, 2008.
23. Zhu Y, Shi YP, Wu D, Ji YJ, Wang X, Chen HL, Wu SS, Huang DJ and Jiang W: Salidroside protects against hydrogen peroxide-induced injury in cardiac H9c2 cells via PI3K-Akt dependent pathway. DNA Cell Biol 30: 809-819, 2011.
24. Tan CB, Gao M, Xu WR, Yang XY, Zhu XM and Du GH: Protective effects of salidroside on endothelial cell apoptosis induced by cobalt chloride. Biol Pharm Bull 32: 1359-1363, 2009.
25. Hu X, Lin S, Yu D, Qiu S, Zhang X and Mei R: A preliminary study: The anti-proliferation effect of salidroside on different human cancer cell lines. Cell Biol Toxicol 26: 499-507, 2010.
26. Chen SF, Tsai HJ, Hung TH, Chen CC, Lee CY, Wu CH, Wang PY and Liao NC: Salidroside improves behavioral and histological outcomes and reduces apoptosis via PI3K/Akt signaling after experimental traumatic brain injury. PLoS One 7: e45763, 2012.
27. Yang ZR, Wang HF, Zuo TC, Guan LL and Dai N: Salidroside alleviates oxidative stress in the liver with non-alcoholic steatohepatitis in rats. BMC Pharmacol Toxicol 17: 16, 2016.
28. In: Guide for the care and use of laboratory animals. th (ed). Washington (DC), 2011.
29. McGrath JC, Drummond GB, McLachlan EM, Kilkenny C and Wainwright CL: Guidelines for reporting experiments involving animals: The ARRIVE guidelines. Br J Pharmacol 160: 1573-1576, 2010.
30. Zhang Y, Li L, Lin L, Liu J, Zhang Z, Xu D and Xiang F: Pharmacokinetics, tissue distribution, and excretion of salidroside in rats. Planta Med 79: 1429-1433, 2013.
31. Perfumi M and Mattioli L: Adaptogenic and central nervous system effects of single doses of 3% rosavin and 1% salidroside Rhodiola rosea L. extract in mice. Phytother Res 21: 37-43, 2007.
32. Feng J, Zhang Q, Mo W, Wu L, Li S, Li J, Liu T, Xu S, Fan X and Guo C: Salidroside pretreatment attenuates apoptosis and autophagy during hepatic ischemia-reperfusion injury by inhibiting the mitogen-activated protein kinase pathway in mice. Drug Des Devel Ther 11: 1989-2006, 2017.
33. Wu L, Zhang Q, Dai W, Li S, Feng J, Li J, Liu T, Xu S, Wang W, Lu X, *et al*: Quercetin pretreatment attenuates hepatic ischemia reperfusion-induced apoptosis and autophagy by inhibiting ERK/NF-κB pathway. Gastroenterol Res Pract 2017: 9724217, 2017.

34. Yang JC, Wu SC, Rau CS, Lu TH, Wu YC, Chen YC, Lin MW, Tzeng SL, Wu CJ and Hsieh CH: Inhibition of the phosphoinositide 3-kinase pathway decreases innate resistance to lipopolysaccharide toxicity in TLR4 deficient mice. J Biomed Sci 21: 20, 2014.
35. Livak KJ and Schmittgen TD: Analysis of relative gene expression data using real-time quantitative PCR and the 2(-Delta Delta C(T)) method. Methods 25: 402-408, 2001.
36. Li J, Xia Y, Liu T, Wang J, Dai W, Wang F, Zheng Y, Chen K, Li S, Abudumijiti H, *et al*: Protective effects of astaxanthin on ConA-induced autoimmune hepatitis by the JNK/p-JNK pathway-mediated inhibition of autophagy and apoptosis. PLoS One 10: e0120440, 2015.
37. Cheng P, Wang F, Chen K, Shen M, Dai W, Xu L, Zhang Y, Wang C, Li J, Yang J, *et al*: Hydrogen sulfide ameliorates ischemia/reperfusion-induced hepatitis by inhibiting apoptosis and autophagy pathways. Mediators Inflamm 2014: 935251, 2014.
38. Li Z, Gao L, Tang H, Yin Y, Xiang X, Li Y, Zhao J, Mulholland M and Zhang W: Peripheral effects of nesfatin-1 on glucose homeostasis. PloS One 8: e71513, 2013.
39. Lv C, Huang Y, Liu ZX, Yu D and Bai ZM: Salidroside reduces renal cell carcinoma proliferation by inhibiting JAK2/STAT3 signaling. Cancer Biomark 17: 41-47, 2016.
40. Hu X, Zhang X, Qiu S, Yu D and Lin S: Salidroside induces cell-cycle arrest and apoptosis in human breast cancer cells. Biochem Biophys Res Commun 398: 62-67, 2010.
41. Mukhopadhyay S, Panda PK, Sinha N, Das DN and Bhutia SK: Autophagy and apoptosis: where do they meet? Apoptosis 19: 555-566, 2014.
42. Clark JM, Brancati FL and Diehl AM: The prevalence and etiology of elevated aminotransferase levels in the United States. Am J Gastroenterol 98: 960-967, 2003.
43. Wang C, Xia Y, Zheng Y, Dai W, Wang F, Chen K, Li J, Li S, Zhu R, Yang J, *et al*: Protective effects of N-acetylcysteine in concanavalin A-induced hepatitis in mice. Mediators Inflamm 2015: 189785, 2015.
44. Zhou Y, Chen K, He L, Xia Y, Dai W, Wang F, Li J, Li S, Liu T, Zheng Y, *et al*: The protective effect of resveratrol on Concanavalin-A-induced acute hepatic injury in mice. Gastroenterol Res Pract 2015: 506390, 2015.
45. Wang HX, Liu M, Weng SY, Li JJ, Xie C, He HL, Guan W, Yuan YS and Gao J: Immune mechanisms of Concanavalin A model of autoimmune hepatitis. World J Gastroenterol 18: 119-125, 2012.
46. Zhang B, Wang Y, Li H, Xiong R, Zhao Z, Chu X, Li Q, Sun S and Chen S: Neuroprotective effects of salidroside through PI3K/Akt pathway activation in Alzheimer's disease models. Drug Des Devel Ther 10: 1335-1343, 2016.
47. Fan XJ, Wang Y, Wang L and Zhu M: Salidroside induces apoptosis and autophagy in human colorectal cancer cells through inhibition of PI3K/Akt/mTOR pathway. Oncol Rep 36: 3559-3567, 2016.
48. Hu L, Zaloudek C, Mills GB, Gray J and Jaffe RB: In vivo and in vitro ovarian carcinoma growth inhibition by a phosphatidylinositol 3-kinase inhibitor (LY294002). Clin Cancer Res 6: 880-886, 2000.
49. Henshall DC, Araki T, Schindler CK, Lan JQ, Tiekoter KL, Taki W and Simon RP: Activation of Bcl-2-associated death protein and counter-response of Akt within cell populations during seizure-induced neuronal death. J Neurosci 22: 8458-8465, 2002.
50. Hart JR and Vogt PK: Phosphorylation of AKT: A mutational analysis. Oncotarget 2: 467-476, 2011.
51. Xu S, Wu L, Zhang Q, Feng J, Li S, Li J, Liu T, Mo W, Wang W, Lu X, *et al*: Pretreatment with propylene glycol alginate sodium sulfate ameliorated concanavalin A-induced liver injury by regulating the PI3K/Akt pathway in mice. Life Sci 185: 103-113, 2017.
52. Gibson EM, Henson ES, Haney N, Villanueva J and Gibson SB: Epidermal growth factor protects epithelial-derived cells from tumor necrosis factor-related apoptosis-inducing ligand-induced apoptosis by inhibiting cytochrome c release. Cancer Res 62: 488-496, 2002.
53. Cardone MH, Roy N, Stennicke HR, Salvesen GS, Franke TF, Stanbridge E, Frisch S and Reed JC: Regulation of cell death protease caspase-9 by phosphorylation. Science 282: 1318-1321, 1998.
54. Liu T, Zhang Q, Mo W, Yu Q, Xu S, Li J, Li S, Feng J, Wu L, Lu X, *et al*: The protective effects of shikonin on hepatic ischemia/reperfusion injury are mediated by the activation of the PI3K/Akt pathway. Sci Rep 7: 44785, 2017.
55. Chen K, Li JJ, Li SN, Feng J, Liu T, Wang F, Dai WQ, Xia YJ, Lu J, Zhou YQ and Guo CY: 15-Deoxy-Δ12,14-prostaglandin J2 alleviates hepatic ischemia-reperfusion injury in mice via inducing antioxidant response and inhibiting apoptosis and autophagy. Acta Pharmacol Sin 38: 672-687, 2017.
56. Zambrano J and Yeh ES: Autophagy and apoptotic crosstalk: Mechanism of therapeutic resistance in HER2-positive breast cancer. Breast Cancer (Auckl) 10: 13-23, 2016.
57. Chen K, Li J, Li S, Feng J, Wu L, Liu T, Zhang R, Xu S, Cheng K, Zhou Y, *et al*: 15d-PGJ2 alleviates ConA-induced acute liver injury in mice by up-regulating HO-1 and reducing hepatic cell autophagy. Biomed Pharmacother 80: 183-192, 2016.
58. Lei F, Chen L, Zhang ZJ and Tian GH: The extraction technology of salidroside and application prospects from rhodiolarosea. Beverage Indust 19: 3, 2016.